3-Oxoisoindoline-1-carboxamides: Potent, State-Dependent Blockers of Voltage-Gated Sodium Channel Na$_V$1.7 with Efficacy in Rat Pain Models

Istvan Macsari,*,[†] Yevgeni Besidski,[†] Gabor Csjernyik,[†] Linda I. Nilsson,[†] Lars Sandberg,[†] Ulrika Yngve,[†] Kristofer Åhlin,[†] Tjerk Bueters,[‡] Anders B. Eriksson,[∥] Per-Eric Lund,[§] Elisabet Venyike,[§] Sandra Oerther,[§] Karin Hygge Blakeman,[§] Lei Luo,[§] and Per I. Arvidsson[∥,⊥,#]

[†]Medicinal Chemistry, [‡]DMPK, [§]Neuroscience, [∥]Project Management, CNSP iMed, AstraZeneca R&D Södertälje, SE-151 85 Södertälje, Sweden

[⊥]Organic Pharmaceutical Chemistry, Department of Medicinal Chemistry, Uppsala Biomedical Centre, Uppsala University, Box 574, SE-751 23 Uppsala, Sweden

[#]School of Pharmacy and Pharmacology, Westville Campus, University of KwaZulu-Natal, Private Bag X54001, Durban 4000, South Africa

Ⓢ *Supporting Information*

ABSTRACT: The voltage-gated sodium channel Na$_V$1.7 is believed to be a critical mediator of pain sensation based on clinical genetic studies and pharmacological results. Clinical utility of nonselective sodium channel blockers is limited due to serious adverse drug effects. Here, we present the optimization, structure−activity relationships, and in vitro and in vivo characterization of a novel series of Na$_V$1.7 inhibitors based on the oxoisoindoline core. Extensive studies with focus on optimization of Na$_V$1.7 potency, selectivity over Na$_V$1.5, and metabolic stability properties produced several interesting oxoisoindoline carboxamides (**16A**, **26B**, **28**, **51**, **60**, and **62**) that were further characterized. The oxoisoindo-line carboxamides interacted with the local anesthetics binding site. In spite of this, several compounds showed functional selectivity versus Na$_V$1.5 of more than 100-fold. This appeared to be a combination of subtype and state-dependent selectivity. Compound **28** showed concentration-dependent inhibition of nerve injury-induced ectopic in an ex vivo DRG preparation from SNL rats. Compounds **16A** and **26B** demonstrated concentration-dependent efficacy in preclinical behavioral pain models. The oxoisoindoline carboxamides series described here may be valuable for further investigations for pain therapeutics.
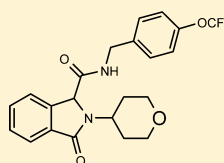
26B

Na$_V$1.7 IC$_{50}$ 0.041 μM (V$_{hold}$ -65 mV)
Na$_V$1.7 IC$_{50}$ 3.8 μM (V$_{hold}$ -90 mV)
Na$_V$1.5 IC$_{50}$ >33 μM
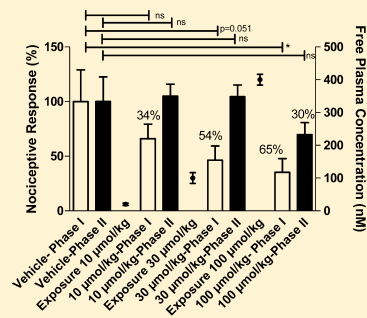
■ INTRODUCTION

The voltage-gated sodium channel Na$_V$1.7 represents an extraordinarily interesting drug target for the treatment of pain. Clinical genetic studies by several groups have established strong genetic links between mutations in the gene SCN9A, coding for Na$_V$1.7 and pain related conditions.[1] Loss of function truncation mutations of SCN9A result in congenital insensibility for pain stimuli, without additional major physiological abnormalities.[2−5] In contrast, gain of function mutations that increase channel opening are known to cause erythermalgia and familial rectal pain, two human inheritable pain conditions.[6−8] Additional support for the potential of voltage-gated sodium channel modulators as pain treatments comes from the notion that a number of clinically used agents developed for other indications, such as mexiletine, lamotrigine, and carbamazepine, showed analgesic activity through nonselective blockade of sodium channels.[9] However, these drugs give rise to serious adverse events in the clinical setting, presumably due to the inhibition of other sodium channels, i.e., Na$_V$1.1−1.9, that influence basal functions in the brain, heart, or muscle. Consequently, much effort has been focused on identifying potent and selective Na$_V$1.7 blockers, which do not inhibit other members of the voltage-gated sodium channel family.[10−17] There are several ways to obtain selectivity between Na$_V$1.7 and other sodium channels. True subtype selectivity for Na$_V$1.7 could be achieved by identifying a unique binding site at Na$_V$1.7 that is not present within other Na$_V$ channels. This is challenging, indeed, because all sodium channel are very similar. An alternative is to develop state-dependent ligands that preferentially bind to the inactivated state of the sodium channels and exploit the difference in kinetic states of different sodium channels in different tissues. It is believed that in hyperexcitable neurons that are an underlying cause for chronic pain, most Na$_V$1.7 channels are inactivated.[18,19]

Scheme 1. Preparation of Oxoisoindoline Carboxamides via Ugi Reaction (Method 1)[a]
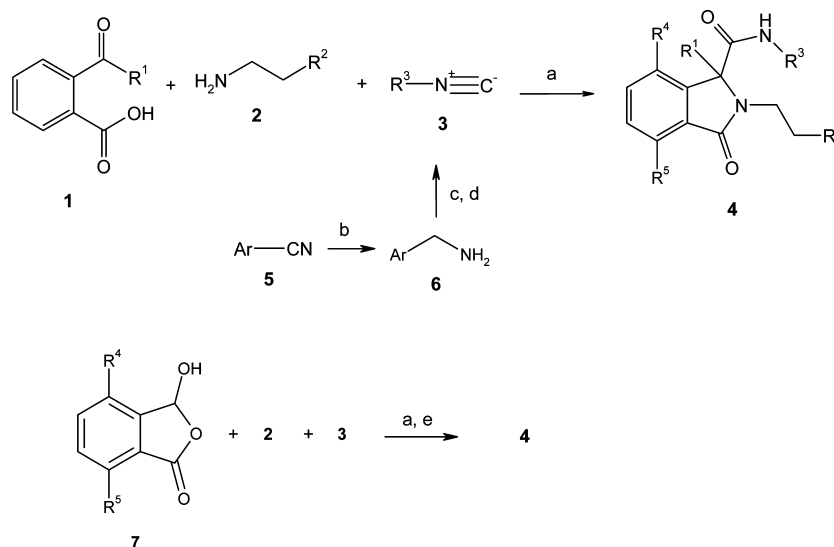
[a]Reagents: (a) MeOH, rt; (b) borane, THF, 60 °C; (c) phenylformate, DCM, 0 °C; (d) POCl$_3$, DIPEA, DCM, −15 °C. R^1 = H, Me; R^2, R^3 = varied; R^4 = H, F, Me, OMe; R^5 = H, F. (e) BBr$_3$, DCM, −78 °C for R^4 = OH.

A combination of subtype selectivity and state dependency could confer compounds that possess sufficient functional selectivity in vivo in order to avoid the adverse effects of the current clinically available nonselective sodium blockers. Herein we present the optimization, structure–activity relationship (SAR), and in vitro and in vivo characterization of a novel series of Na$_V$1.7 inhibitors based on the oxoisoindoline core.

CHEMISTRY

The synthesis of oxoisoindoline carboxamides (**4**) is based upon the three component Ugi reaction and outlined in Scheme 1. Acid **1**, amine **2**, and isocyanide **3** were mixed in methanol and stirred at room temperature overnight to afford the desired products.[20−23] The method was general, and a wide range of amines and isocyanides could be used in a library fashion to prepare the desired molecules. The commercial availability of functionalized aryl isocyanides is limited, therefore a short sequence starting from the appropriate aryl nitrile (**5**) was devised. The amines **6** were prepared by reduction of **5** and then subjected to formylation and water elimination reactions in order to obtain the functionalized isocyanides **3**.

The synthesis of substituted isooxindoles was also achieved by the above-mentioned Ugi reaction (Scheme 1) employing 4- or 7-substituted isobenzofuranones (**7**), which were prepared by published methods.[24,25] Fluoro, methyl, and methoxy groups were introduced using this approach. Moreover, demethylation of methoxy moiety afforded the phenol derivative of **4**.

An alternative method to the Ugi reaction was also developed, as depicted in Scheme 2.[20−23] The diester **8** was brominated in the benzylic position and then reacted with the appropriate amine **2** to form the oxoisoindoline ring, followed by hydrolysis of the ester intermediate.[26] The acid **9** was reacted with benzyl amine **6** to afford the product amide **4**. This method made it possible to avoid the use of poisonous isocyanide reagent. On the other hand, acid **9** proved to be very unreactive in the amidation reaction and only via the very sensitive acid fluoride could the coupling be achieved.

Scheme 2. Preparation of Oxoisoindoline Carboxamides via Amide Coupling (Method 2)[a]
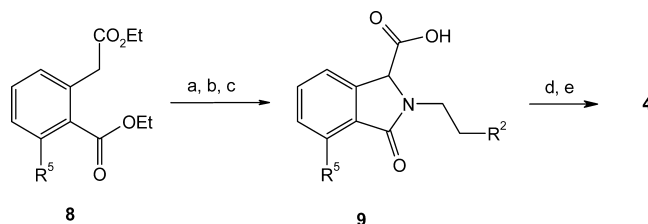
[a]Reagents: (a) NBS, AIBN, CCl$_4$, reflux; (b) **2**, TEA, acetonitrile, 0 °C; (c) 1 M NaOH, MeOH, rt; (d) **6**, fluoro-N,N,N',N'-tetramethylformamidinium hexafluorophosphate, TEA, DMF, 45 °C. R^5 = H, OMe. (e) BBr$_3$, DCM, −78 °C for R^5 = OH.

BIOLOGICAL EVALUATION

Oxoisoindoline carboxamides were initially identified as blockers of the human Na$_V$1.7 channel, recombinantly expressed in HEK 293 cells, using a Li flux atomic absorption spectroscopy (AAS) assay.[27] Potency of identified and synthesized compounds was determined by automated perforated whole-cell patch clamp using the automated IonWorks instrument, mainly with a steady-state protocol (V_{hold} −65 mV), which is physiologically relevant to the conditions in C-type dorsal root ganglion neurons.[28,29] Analogues were further examined for their selectivity mainly over the human Na$_V$1.5 channel using a physiologically relevant assay with a V_{hold} of −90 mV.[30,31] In addition, selectivity over the hERG channel as well as analysis of state-dependent properties of the compounds on Na$_V$1.7 was determined. Mode of action studies were conducted on a point-mutated channel where one of the key amino acid residues of the local anesthetic binding site was changed (F1737A). Furthermore, key compounds were tested against a broader panel of mainly CV and CNS liability targets. Finally, on the basis of their potency, selectivity, and pharmacokinetic profiles, compounds were evaluated for analgesic efficacy using ex vivo and in vivo models of inflammatory and neuropathic pain. These studies include ex vivo effects of L5/L6 spinal nerve ligation-induced (Chung) ectopic activity, in vivo behavioral effects in the formalin model of

peripherally driven spontaneous pain, and the carrageenan-induced monoarthritis model of chronic inflammatory pain.

■ RESULTS AND DISCUSSION

During the course of our $Na_V1.7$ blocker program, we identified a series of oxoisoindoline carboxamides from a targeted library represented by compound **10** (Figure 1). Analysis of the library
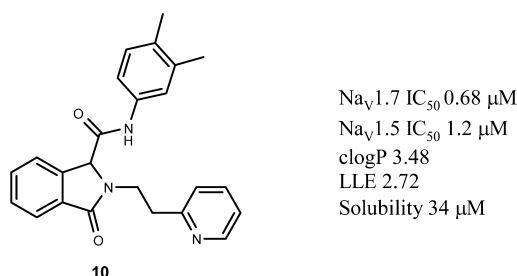

$Na_V1.7$ IC_{50} 0.68 μM
$Na_V1.5$ IC_{50} 1.2 μM
clogP 3.48
LLE 2.72
Solubility 34 μM

10

Figure 1. Profile of oxoisoindoline carboxamide hit **10**. LLE, lipophilic ligand efficiency, is calculated as $Na_V1.7$ pIC_{50} − clogP.

showed that close analogues to **10** with medium $Na_V1.7$ potency (IC_{50} < 0.5 μM) all possessed an *ortho* disubstituted aniline group regardless of the side chain. Those compounds showed very poor solubility, typically around or below 1 μM. We were particularly pleased to see that **10**, which does not have a substituent in the *ortho* position, was associated with improved solubility. However, **10** showed modest in vitro $Na_V1.7$ potency and no selectivity over $Na_V1.5$, as measured in whole-cell voltage clamp electrophysiology assays.[31] Good $Na_V1.5$ selectivity is an absolute requirement for further development of a potential drug candidate, as this sodium channel is widely expressed in the heart muscle and its inhibition leads to ventricular arrhythmia.[32,33] These initial findings prompted us to conduct further investigations aimed to identify compounds with higher $Na_V1.7$ potency and increased selectivity toward $Na_V1.5$. CNS exposure was not in the scope of the optimization because the expression of the $Na_V1.7$ protein suggests a peripheral mechanism of action.

In our first attempt to optimize the series, we focused our attention on replacing the aniline group, which could become a toxicity liability if the amide function is hydrolyzed in vivo. Because the dialkyl substituted aniline moiety in **10** is well tolerated, replacement with a benzyl amine moiety should potentially be possible due to similar steric demand. We initially decided to design and prepare analogues to **10** with variations of the amide part. The results of 13 synthesized analogues are summarized in Table 1.

Our hypothesis proved to be correct as compound **11** retained $Na_V1.7$ potency in the steady state protocol (vide infra) and even increased the selectivity somewhat over $Na_V1.5$. The isomeric **12** was as potent as **11**, but the bromo atom in the *ortho* position (**13**) was not tolerated. The trifluoromethyl group (**14**) helped to further increase the $Na_V1.7$ potency (cf. **10**), whereas the $Na_V1.5$ blocking activity was retained. The electron donating methoxy group (**15**) did not influence $Na_V1.7$ potency but considerably lowered the $Na_V1.5$ activity, thereby improving selectivity. In **16** and **17**, the introduction of trifluoromethoxy group increased the $Na_V1.7$ potency and, similarly to **14**, did not considerably influence the potency to the $Na_V1.5$ channel. The replacement of the trifluoromethyl group with the trifluoroethyl functionality in **18** gave a similarly potent compound as **14**. Further elongation of the chain in **19** helped only to lower the $Na_V1.5$ potency (cf. **16**). The introduction of the methyl group in
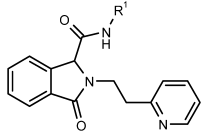
20 was tolerated but did not significantly influence the potency (cf. **19**). The phenyl ring was replaced by a pyridine ring in compounds **21**−**23**. This type of moiety was successfully incorporated in other in-house series of $Na_V1.7$ channel blockers.[14] Unfortunately, the potency was lower compared to the corresponding phenyl analogues (**21** and **22**, cf. **16** and **19**). On the other hand, the selectivity over $Na_V1.5$ was improved. These pyridine-containing compounds also showed an improved in vitro metabolic stability profile compared to the other analogues presented in Table 1, presumably, at least partly, due to lower lipophilicity. Particularly, the metabolic stability in human liver microsomes for most other analogues was too high and required additional optimization in order to meet the desired profile of once or twice daily dosing in human.
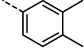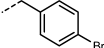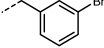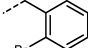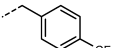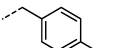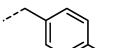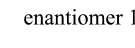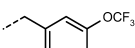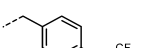
In general, the *meta* and *para* substituted benzyl amides were equally well tolerated (**11**, **12**, **16**, and **17**). Small groups such as trifluoromethyl (**14**) and trifluoromethoxy (**16**, **17**) had the highest positive influence on the $Na_V1.7$ potency. Alkoxy (**15**) or trifluoroalkoxy groups, especially in case of pyridines **21**−**23**, helped to lower the $Na_V1.5$ potency. The solubility was generally good for most of the benzyl amides, the exception being **12** and **14**, where the solubility dropped below 10 μM. The analyzed compounds blocked the hERG channel with potencies between 7 and 20 μM.

Compound **16** showed an attractive profile due to good $Na_V1.7$ potency and in vitro microsomal stability in rat compared to close analogues (Table 1). Therefore, we decided to study this compound further. The enantiomers were separated and tested; however, the absolute stereochemistry could not be determined, and instead the first eluting enantiomer from the chiral HPLC column was labeled A and the second eluting enantiomer was labeled B. We w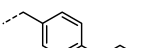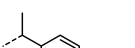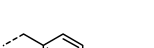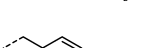ere pleased to see that enantiomer 1 (**16A**) showed 56 nM potency against $Na_V1.7$ (Table 1, cf. **16**). For the less active enantiomer 2 (**16B**), a potency value of 1.4 μM was determined. The pharmacokinetic profile of **16A** in rat is summarized in Table 2. Following intravenous administration, the plasma concentration of **16A** increased slightly from 6 to 24 h due to redistribution or reabsorption. This explained the large volume of distribution. The clearance was approximately 40% of plasma liver blood flow, which correlated well to the observed metabolic stability in vitro. The oral pharmacokinetics demonstrated rapid absorption, good exposure, and bioavailability. Encouraged by the favorable pharmacokinetic properties in rodents, and with the high hERG affinity and low human liver microsome stability in mind, **16A** appeared a good preclinical tool compound. It was also used as a starting point for further optimizations.

Next, we decided to probe the effects of the side chain modifications on the SAR. The generated results are summarized in Table 3. Replacement of the pyridine ring of **16** by tetrahydropyran (**24**) and morpholine (**25**) mainly lowered the $Na_V1.5$ channel potency. Surprisingly, the removal of the chain in **26** gave an equipotent compound to **24**. The enantiomers of **26** showed different blocking activity on the 1.7 channel, as we have previously seen for **16** (Table 1). Furthermore, the contraction of the ring to tetrahydrofuran (**27**) was well tolerated. When the oxygen atom of **26** was replaced by a −CF_2 group in **28**, the $Na_V1.7$ potency increased. It is interesting to note the ∼70-fold difference in potency against the $Na_V1.7$ channel between the two enantiomers (**28A,B**). A cyano group (**29**) or carbamate function (**30**) were not beneficial in this position. The introduction of the smaller azetidine and cyclobutyl rings in **31**−**33** retained $Na_V1.7$ potency, cf. **28**. When the ring was

Table 1. The Effect of SAR around the Variation of Amide Part

Entry	R^1	$Na_V1.7^a$ IC$_{50}$ (μM)	$Na_V1.7^b$ IC$_{50}$ (μM)	$Na_V1.5^b$ IC$_{50}$ (μM)	hERG IC$_{50}$ (μM)	Solubility^c (μM)	RLM/HLM Cl$_{int}$ (μl/min/mg)
10		0.68	2.3	1.2	ND	34	ND/ND
11		0.35	ND	8.7	9.3	57	31/120
12		0.35	ND	12	ND	6	47/310
13		>11	ND	>33	ND	280	20/300
14		0.17	0.82	1.6	8.6	7	58/180
15		1.6	ND	>23	ND	360	ND/ND
16		0.16	0.41	1.2	7.8	13	24/292
16A	enantiomer 1	0.056	0.08	0.73	4.6	26	<10/98
16B	enantiomer 2	1.4	ND	18	ND	27	<10/130
17		0.049	0.22	2.8	21	19	86/370
18		0.26	ND	4.4	14	120	42/190
19		0.36	0.94	8.9	8.9	42	ND/ND
20		0.55	1.4	3.7	7.3	34	49/204
21		1.9	>10.5	>33	ND	32	<10/33
22		0.34	2.3	>33	16	88	<10/40
23		0.45	ND	>33	20	110	<10/39

^{a} V_{hold} −65 mV. ^{b} V_{hold} −90 mV. ^{c} Dried DMSO solubility, ref 34. ND, not determined.

replaced by short aliphatic chains in **34−37**, somewhat decreased Na$_V$1.7 potencies, cf. **16**, were observed.

Unfortunately, the Na$_V$1.7 potency was negatively influenced by the introduction of smaller aliphatic chains and rings, the exceptions being **28**, **31** and **32**. On the positive note, the Na$_V$1.5 affinity was significantly lowered in most cases, which led to an increased selectivity window (up to 100 times). Furthermore, the solubility improved with a few exceptions (**28**, **32**, **33**, and **35**) and the hERG potency was lowered. The good metabolic stability in rat was also retained and in human significantly

Table 2. Rat in Vivo PK for 16A, 26B, 28, 51, 60, and 62

	16A	26B	28	51	60	62
AUC^a (h·μmol/L)	1.7	1.7	2.4	1.4	2.1	1.6
V_{ss}^a (L/kg)	7.6	0.8	5.2	1.1	0.7	0.9
$t_{1/2}^a$ (h)	0.8	1.0	4.1	0.4	0.4	0.4
CL^a (mL/min/kg)	29	30	21	37	29	32
AUC^b (h·μmol/L)	2.1	1.1	6.5	2.1	0.4	0.2
C_{max}^b (μmol/L)	0.6	0.6	0.5	0.8	0.09	0.1
t_{max}^b (h)	0.5	0.3	3.7	0.3	0.4	0.3
$t_{1/2}^b$ (h)	5.9	1.9	5.9	2.3	8.1	1.2
F^b (%)	37	20	80	44	6	4
f_u (% free)	4.5	13.2	3.0	9.2	18.0	13.0

^{a}Intravenous (iv), dose 3 μmol/kg. ^{b}Per oral (po), dose 10 μmol/kg.

improved. This suggested that the ethylpyridine moiety was associated with a metabolic soft-spot, particularly in human microsomes. Subsequent biotransformation studies showed that this moiety was indeed oxidized at several locations. In summary, compound **26B** and **28** showed the most attractive overall profile. The pharmacokinetics of **26B** and **28** in rat are summarized in Table 2. Particularly, the long-lasting exposure and high bioavailability of **28** after 10 μmol/kg po was of interest. To allow administration of larger doses, however, the formulation had to be changed from a solution-based to a suspension-based one. The total AUC in rat was reduced 3-fold to 2 h·μmol/L and the C_{max} 2-fold to 0.3 μmol/L after 30 μmol/kg per oral dosing with a suspension-based formulation compared to the 10 μmol/kg dose given as a solution, presumably caused by the low solubility of **28**. This impeded additional in vivo studies with **28**. Therefore, **26B**, which had significantly higher solubility than **28** and similar PK profile as **16A**, was chosen for further studies (vide infra).

At this point in our investigation, we turned our attention to design and prepare close analogues to the ethyl pyridine side chain of **16** to investigate primarily if the human metabolic stability could be improved. The generated results are summarized in Table 4. The isomeric pyridines (**38** and **39**, cf. **16**) were tolerated, **39** being the least active. The introduction of small substituents on the ring, such as fluoride (**40**) and methyl (**41**), retained the Na$_V$1.7 potency. In the case of compounds **42**−**44**, the chain length was varied; elongation was well tolerated (**42** and **43**) but not shortening (**44**). When a methyl substituent was introduced on the chain, the Na$_V$1.7 potency was retained in **45** and **46**, however, decreased by 10 times in case of **47**. On the positive note, difluoro substitution of the chain (**48**) increased the Na$_V$1.7 potency. Replacement of the pyridine ring with a pyrimidine (**49**) and pyridazine (**50**) decreased the Na$_V$1.7 blocking activity. The *para* fluoro substitution in **51** increased the potency, cf. **49**.

In general, the good Na$_V$1.7 potency was retained throughout the subseries. Furthermore, the Na$_V$1.5 potency was decreased in all cases, except for **38**, **40**, **41**, and **48**. The solubility was improved for most compounds, the exceptions being **40**−**44**, **46**, and **47**. A few possibilities were identified that improved the metabolic stability in human microsomes. Removal (**44**) or disubstitution (**47**−**48**) of the α-C carbon in the ethyl chain diminished oxidative metabolites. Also, replacement of pyridine by pyrimidine reduced oxidative metabolism. However, the potency for the hERG channel was retained, or slightly increased, for all compounds with the exception of **49**. We would like to highlight compound **51**, which showed an attractive profile with

high selectivity over the Na$_V$1.5 channel and good metabolic stability measured in rat liver microsomes.

The oxoisoindoline carboxamides contain a chiral center and are prone to racemization due to the acidity of the proton. Therefore, a methyl group was introduced into the quaternary center (**52**, in Table 5) and the enantiomers were separated by chiral HPLC. We found that the enantiomers showed different potency for the Na$_V$1.7 channel similarly to **16**, **26**, and **28** (IC$_{50}$ = 3.6 μM for **52A** and IC$_{50}$ = 0.17 μM for **52B**). The absolute configurations were not determined. In comparison to **16**, the racemic **52** showed decreased potency but increased selectivity against Na$_V$1.5. Unfortunately, both solubility and metabolic stability were dramatically decreased.
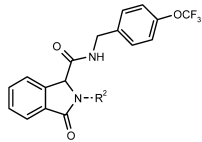
To gain further insight to the structure−activity relationship in the series, different functional groups were introduced on the oxoisoindoline core (see Table 5). Replacement of the proton in the 7 position (R^4) with fluoride atom (**53**), methyl (**54**), and methoxy (**55**) functionalities were well tolerated. However, a hydroxyl group (**56**) lowered the Na$_V$1.7 potency. Among the modifications in the 4 position (R^5, **57**−**59**), all except the methoxy functional group was tolerated (**58**). The Na$_V$1.5 potency was decreased in all cases, except in **53** and **59**. Unfortunately, the solubility was very poor for all compounds, with exceptions for **53**, **57**, and **59**. Furthermore, the affinity to the hERG channel increased somewhat with only one exception (**57**) and the metabolic stability was lower throughout the series. In summary, the fluoro atom in the 7 and the hydroxyl group in the 4 position only led to compounds which showed similar properties as **16** but provided no clear advantages.
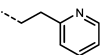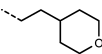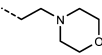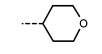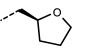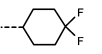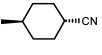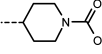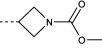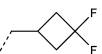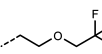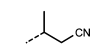
At this point, we turned our attention again on compound **51**, which showed an attractive profile with high selectivity over Na$_V$1.5 channel and good metabolic stability measured in rat liver microsomes (Table 4). We decided to design and prepare a few analogues to **51** to improve selectivity against the hERG channel among others. The generated results are shown in Table 6. In **60**, the trifluoromethoxy group in the *meta* position (R^7) was tolerated as previously seen for **17** (Table 1). Furthermore, disubstituted **61** and **62** also retained the good potency. The hydroxyl group in R^5 (**63**) slightly increased the Na$_V$1.7 activity, as seen in **59** (see Table 5). The selectivity over Na$_V$1.5 was retained for all compounds. The solubility increased in case of **60** and was very poor in **63**. Compounds **60** and **62** showed significantly lower potency for the hERG channel than **51**.

The overall profiles of **60** and **62** were promising, and rat pharmacokinetics were determined together with **51** (Table 2). When administered intravenously, all three compounds showed very similar profiles. The oral PK profile of **51** was similar to **16A**. However, in the cases of **60** and **62**, low exposure and bioavailability were measured. Surprisingly, the good in vitro metabolic stability in rat for **60** and **62** did not translate well to good overall in vivo PK data. The low bioavailability of **60** and **62** could not be explained by systemic metabolism or poor permeability. The clearance after iv administration was approximately 40% of plasma liver blood flow, similarly to **16** or **51**. Also, in vitro permeability determined in CaCo2 cells was excellent for these compounds, 50×10^{-6} and 39×10^{-6} cm/s for **60** and **62**, respectively. Possible explanations are presystemic metabolism, instability, or precipitation in the rat gut. Although these compounds might still have acceptable pharmacokinetics in human based on scaling, poor rodent PK poses a great hurdle in the further development of such compounds.
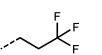
Of the 23 compounds with a Na$_V$1.7 potency below 0.2 μM, seven compounds (**28A** and **B**, **43**, **46**, **52B**, **55**, **60**, and **61**)

Table 3. SAR of Replacements of Ethyl Pyridine Chain
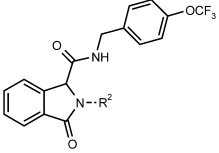
Entry	R^2	Na$_V$1.7[a] IC$_{50}$ (μM)	Na$_V$1.7[b] IC$_{50}$ (μM)	Na$_V$1.5[b] IC$_{50}$ (μM)	hERG IC$_{50}$ (μM)	Solubility[c] (μM)	RLM/HLM Cl$_{int}$ (μl/min/mg)
16		0.16	0.41	1.2	7.8	13	24/292
24		0.32	ND	19	22	20	<10/71
25		0.71	2.0	2.9	ND	200	<10/49
26		0.37	ND	>33	>33	28	<10/14
26A	enantiomer 1	2	ND	>33	ND	83	ND/ND
26B	enantiomer 2	0.41	3.8	>30	>33	83	<10/15
27		0.52	25	>33	17	28	28/50
28		0.11	ND	14	14	<4	15/20
28A	enantiomer 1	6.9	ND	>33	ND	5	10/10
28B	enantiomer 2	0.092	1.0	>31	>33	3	13/27
29		0.57	2.5	6.1	>33	200	11/<10
30		0.33	2.2	4.5	14	7	89/170
31		0.11	2.2	4.4	11	30	<10/43
32		0.19	8.5	12	23	4	<10/15
33		0.53	ND	18	ND	<1	38/25
34		0.42	6.6	19	ND	11	<10/<10
35		0.75	ND	>33	ND	3	<10/44
36		0.43	10	>31	31	70	<10/<10
37		0.89	11	>26	26	45	16/11
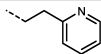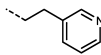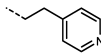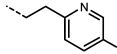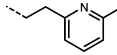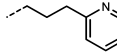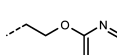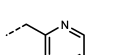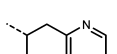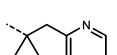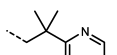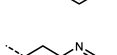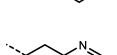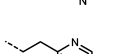
[a]V_{hold} −65 mV. [b]V_{hold} −90 mV. [c]Dried DMSO solubility, ref 34. ND, not determined.

display functional selectivity over Na$_V$1.5 by 100-fold or more (Table 3−6). This is a significant improvement of Na$_V$1.5 selectivity compared to clinically used compounds. Two well

characterized and potent Na$_V$1.7 blockers, tetracaine and amitriptyline, were used for comparison.[35] They displayed only 2−5-fold difference in potency between Na$_V$1.7 and 1.5 (Table

Table 4. SAR of Heterocyclic Ring Variations
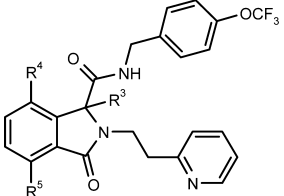
Entry	R^2	$Na_V1.7^a$ IC$_{50}$ (μM)	$Na_V1.7^b$ IC$_{50}$ (μM)	$Na_V1.5^b$ IC$_{50}$ (μM)	hERG IC$_{50}$ (μM)	Solubility^c (μM)	RLM/HLM Cl$_{int}$ μl/min/mg
16		0.16	0.41	1.2	7.8	13	24/292
38		0.19	ND	2.6	5.5	69	28/100
39		0.31	ND	6.1	5.1	61	20/170
40		0.16	ND	1.2	5.3	5	110/300
41		0.073	0.37	1.9	6.6	3.5	72/380
42		0.13	4.6	7.9	ND	6	31/>500
43		0.082	18	9.7	4.9	<1	39/190
44		0.43	ND	4.3	3.3	<1	35/39
45		0.15	ND	4	8.6	28	<10/82
46		0.097	5.7	13	4.3	13	67/340
47		1.6	ND	>25	ND	6	<10/40
48		0.045	0.52	1.9	9.7	2	30/57
49		0.55	1.6	>8.3	16	310	<10/33
50		0.38	1.9	12	9.2	12	ND/161
51		0.23	ND	19	5.5	25	<10/53

$^a V_{hold}$ −65 mV. $^b V_{hold}$ −90 mV. ^{c}Dried DMSO solubility, ref 34. ND, not determined.

7). The functional selectivity is to the largest extent achieved through increased state-dependent properties, e.g., compounds **43**, **52B**, and **55** show more than 100-fold difference between the resting-state (V_{hold} −90 mV) and the steady-state (V_{hold} −65 mV) protocols, reflecting preferential affinity for the inactivated versus resting state of the $Na_V1.7$ channel. This is largely in agreement with what has been reported for other recently described $Na_V1.7$ blockers.[12] Although state-dependent properties have also been observed with clinically used sodium channel blockers such as local anesthetics, anticonvulsants, and
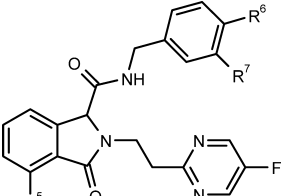
Table 5. The Effect on SAR around Core Modifications

entry	R^3	R^4	R^5	$Na_V1.7^a$ IC_{50} (μM)	$Na_V1.7^b$ IC_{50} (μM)	$Na_V1.5^b$ IC_{50} (μM)	hERG IC_{50} (μM)	solubility[c] (μM)	RLM/HLM Cl_{int} (μL/min/mg)
16	H	H	H	0.16	0.41	1.2	7.8	13	24/292
52	Me	H	H	0.88	ND	>31	ND	<1	57/>500
52A	Me	H	H	3.6	ND	27	ND	20	ND/ND
52B	Me	H	H	0.17	21	25	11	20	ND/ND
53	H	F	H	0.087	0.28	0.81	5.6	17	10/150
54	H	Me	H	0.051	0.18	4.7	5.6	1	59/190
55	H	OMe	H	0.16	22	16	3.6	4	37/97
56	H	OH	H	0.40	>33	>33	ND	<1	23/26
57	H	H	F	0.29	1.7	17	8.2	26	16/170
58	H	H	OMe	3.1	ND	8.5	ND	6	<10/50
59	H	H	OH	0.064	ND	0.94	ND	15	10/59

$^a V_{hold}$ −65 mV. $^b V_{hold}$ −90 mV ^{c} Dried DMSO solubility, ref 34. ND, not determined.

Table 6. SAR of Analogues of 51

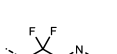| entry	R^5	R^6	R^7	$Na_V1.7^a$ IC_{50} (μM)	$Na_V1.7^b$ IC_{50} (μM)	$Na_V1.5^b$ IC_{50} (μM)	hERG IC_{50} (μM)	solubility[c] (μM)	RLM/HLM Cl_{int} (μL/min/mg)
51	H	OCF$_3$	H	0.23	ND	19	5.5	25	<10/53
60	H	H	OCF$_3$	0.13	0.78	>16	24	61	28/180
61	H	F	OCF$_3$	0.14	ND	17	ND	27	110/220
62	H	F	CF$_3$	0.22	0.99	>25	>33	14	<10/<10
63	OH	OCF$_3$	H	0.14	ND	>10	ND	2	36/42

$^a V_{hold}$ −65 mV. $^b V_{hold}$ −90 mV. ^{c} Dried DMSO solubility, ref 34. ND, not determined.

Table 7. In Vitro Profile of 16A, 26B, 28B, 60, 62, Amitriptyline, and Tetracaine

entry	$Na_V1.7^a$ IC_{50} (μM)	$Na_V1.7^b$ IC_{50} (μM)	$Na_V1.7^a$ (F1737A) IC_{50} (μM)	$Na_V1.5^b$ IC_{50} (μM)	$Na_V1.2^a$ IC_{50} (μM)
16A	0.053	0.083	10	0.73	8.1
26B	0.41	3.8	>33	>30	>33
28B	0.092	1.0	>10	>31	>33
60	0.13	0.78	ND	>16	>33
62	0.23	0.99	33	>25	>33
amitriptyline	1.0	7.0	12	1.6	3.1
tetracaine	0.11	0.62	33	0.53	1.1

$^a V_{hold}$ −65 mV. $^b V_{hold}$ −90 mV. ND, not determined.

antiarrhythmics, the absolute differences in the potency between compounds such as tetracaine and amitriptyline are less pronounced than that for the described oxoisoindoline carboxamides (Table 1, 3−7).

Selected compounds were also evaluated for their activity on one of the major brain sodium channels, $Na_V1.2$. Table 7 shows

the properties of **16A**, **26B**, **28B**, **60**, and **62** as well as tetracaine and amitriptyline. Interestingly, the most $Na_V1.5$ selective compounds (**28B**, **60**, and **62**) showed no inhibition of $Na_V1.2$ at 33 μM. For comparison, tetracaine and amitriptyline inhibited $Na_V1.2$ with IC_{50} of 1.1 and 3.1 μM, respectively. In depth electrophysiological studies are required to understand the mechanism of action of the described compounds as well as the absolute selectivities versus the different sodium channels.

In vitro selectivities for compound **16A** and **26B** were determined in functional or radioligand bindings assays. In functional ion channel assays, using either IonWorks or FLIPR, compound **26B** was inactive at 10 μM on the potassium channels $K_V1.5$, KCNQ2, at 33 μM on hERG, hIKs, and at 31.6 μM on the calcium channel $Ca_V3.2$. The more $Na_V1.7$ potent compound, **16A**, blocked the potassium channels: hERG, $K_V1.5$, and KCNQ2 with IC_{50}s of 4.6, 1.5, and 1.6 μM, respectively, but was inactive on IKs at 33 μM. In addition, this compound inhibited at 31.6 μM the calcium channel $Ca_V3.2$ by 44%. Both compounds were inactive on the ligand-gated channels TRPA1 (at 11 μM) and glycine receptor α1 (at 33 μM). As determined by radioligand binding, no activity was detected at 10 μM for a

panel of 20 targets at MDS pharma.[36] At $10\,\mu M$, compounds **16A** and **26B** inhibited the binding of [³H]batrachotoxin (sodium channel, site 2) to rat brain membranes by 100% and 79%, respectively, indicating overlapping binding to the local anesthetic binding site.

The binding epitope for local anesthetics is mostly formed by residues in the sixth transmembrane segments mainly of the third and fourth domains of the sodium channel peptide sequence.[37] We further sought to understand the site of binding by site-directed mutagenesis of phenylalanine 1737 to alanine in the $Na_V1.7$ channel followed by functional analysis. The potency of compounds **16A**, **28B**, and **62** for the mutated channel was reduced by ∼100-fold (Table 7). For comparison, the potency of amitriptyline was reduced by ∼12-fold and tetracaine by >300-fold, which is in agreement with previous studies.[38,39] These results demonstrate that the oxoisoindoline carboxamides most likely bind to the local anesthetic site of the $Na_V1.7$ channel.

Prior to efficacy studies in rat models of pain, the potencies of selected compounds were determined on recombinantly expressed rat $Na_V1.7$ channels. For the majority of compounds, less than 3-fold difference between rat and human $Na_V1.7$ was observed, which is not a surprise because the channels are evolutionary well conserved. The ability of compound **28B** to inhibit SNL-induced ectopic activity in a rat DRG ex vivo preparation was investigated. The in vitro potency on the rat $Na_V1.7$ channel as measured by whole cell electrophysiology using a steady-state protocol (V_{hold} −65 mV) was determined to be 74 nM, which was selected as the lowest test concentration. Compound **28B** caused a progressive inhibition of the ectopic firing and reached more than 50% inhibition in 6 out of 11 analyzed fibers. The responding fibers displayed a baseline firing frequency of 9.38 ± 1.96 Hz (mean ± SEM), which was used for calculation of the dose-dependent efficacy. At 222 and 740 nM, compound **28B** caused 45.8 ± 13.4% and 82.3 ± 9.6% inhibition (mean ± SEM, $n = 6$) of the SNL-induced ectopic firing, respectively (Figure 2). Thus, the estimated EC_{50} for ex vivo
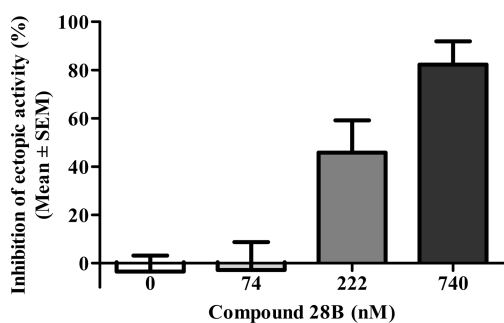

Figure 2. Concentration-dependent effects of compound **28B** on ectopic firing from injured DRG neurons. Buffer or compound **28B** at 74, 222, and 740 nM were perfused cumulatively on DRGs excised from SNL rats at 15 min for each concentration. The effects during the last 3 min were analyzed and expressed as % inhibition (mean ± SEM, $n = 6$).

inhibition of SNL-induced ectopic is ∼3-fold for the in vitro $Na_V1.7$ potency of the compound. Unfortunately, due to low solubility of **28B**, further in vivo analysis of this compound was stopped.

On the basis of the physicochemical properties and on the in vitro potency on the $Na_V1.7$ channel, both compounds **16A** and **26B** were selected to assess their in vivo efficacy in the rat formalin model and carrageenan monoarthritis model. The formalin model is a peripherally driven model with components

of central sensitization.[40] It measures spontaneous rather than evoked pain responses. Clinical conditions triggered by activation of $Na_V1.7$ are erythromelalgia and paroxysmal extreme pain disorder. They are considered to be spontaneous pain disorders and are likely to be peripherally driven.[2] In the formalin model, the first phase (0−5 min) is more peripherally driven than the second phase (15−35 min). In carrageenan-induced monoarthritis, a unilateral inflammation is induced and change in gait pattern is recorded. The reason for using a small and unilateral joint is that it may reflect the inflammatory process seen in patients with rheumatoid arthritis, a disease that usually starts in small joints.[41,42]

The rat $Na_V1.7$ potency, using a steady-state protocol (V_{hold} −65 mV), for compounds **16A** and **26B**, was determined to be 0.074 and $1.6\,\mu M$, respectively. As seen in Figure 3, compound **16A** showed dose-dependent efficacy in the formalin model, with statistically significant analgesic effects in both phase I and II. In phase I, there was a significant effect at $140\,\mu mol/kg$ and in phase II from $30\,\mu mol/kg$ with dose-relevant trends even at lower doses. In the carrageenan model (Figure 5), there was a significant reduction in the pain behavior by 42% at $100\,\mu mol/$ kg. Figure 4 shows that compound **26B** displayed a dose- and concentration-dependent inhibition of painful behavior that reached statistical significance at the highest dose tested ($100\,\mu mol/kg$) in phase I of the formalin model. The same dose of **26B** resulted in a 42% reduction in pain behavior in the carrageenan model, although this did not reach statistical significance (p value = 0.068; Figure 6). For both compounds, no visual side effects have been observed under the time the tests were performed. Free plasma concentrations of 100 and 400 nM were achieved at the end of the formalin experiment for compounds **16A** and **26B**, respectively, which is 0.7−4-fold the measured in vitro IC_{50} values for the rat $Na_V1.7$ channel. The brain:plasma ratio was 2−5 for compound **16A** and 1−2 for compound **26B**, indicating that both compounds have unrestricted access to the brain. The efficacies seen with compounds **16A**, **26B**, and **28B** in the different rat ex vivo and in vivo models could, in addition to inhibition of $Na_V1.7$, be due to blockade of, e.g., $Na_V1.3$ and/or $Na_V1.8$. Further studies are required to fully understand the mechanism behind the effects of the described oxoisoindoline carboxamides.

■ CONCLUSION

In conclusion, a high-throughput screening campaign using a functional ion-flux assay identified compound **10** as a nonselective, state-dependent blocker of $Na_V1.7$. An extensive structure−activity relationship evaluation with focus on optimization of $Na_V1.7$ potency, selectivity over $Na_V1.5$, and metabolic stability properties produced several interesting oxoisoindoline carboxamides that were further characterized. A potent and selective compound **28B** showed concentration-dependent inhibition of nerve injury-induced ectopic in an ex vivo DRG preparation. Two compounds, **16A** and **26B**, with good PK properties in rat demonstrated dose and exposure dependent efficacy in preclinical pain models. Compound **26B** showed selectivity over several ion channels and GPCRs. Binding of the oxoisoindoline carboxamides to the local anesthetics site of the $Na_V1.7$ channel was further demonstrated. Despite this, several compounds showed functional selectivity over $Na_V1.5$ by more than 100-fold. The selectivity is likely achieved in combination of the state-dependent properties of the compounds with interactions to nonconserved amino acid residues outside of the local anesthetics site. The oxoisoindoline
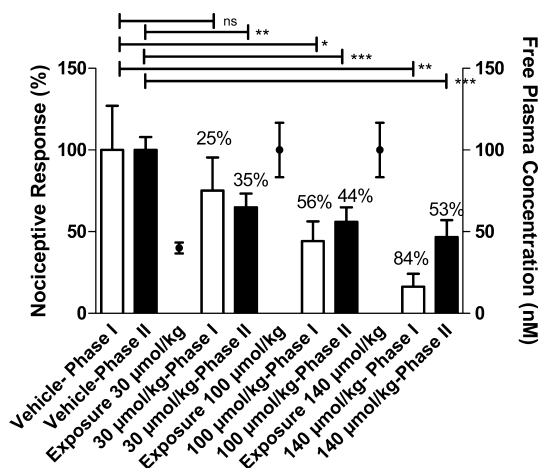
Figure 3. Dose response effect of **16A** in the rat formalin model. Compound is administered per oral gavage 15 min before formalin (100 μL of 2% solution) injection into the dorsal paw of Sprague−Dawley rats. Dose response effect is represented for both phases of the formalin test (phase I, 0−5 min; phase II, 15−35 min post formalin injection). The effect is expressed as the percentage in comparison to vehicle treated group ($n = 9$ per group) and free plasma concentration is expressed as mean ± SEM ($n = 9$ per group). Pairwise comparisons are used as t tests (Bonferroni) within a one-Way ANOVA model per phase. No adjustment is performed for multiple comparisons. $*p < 0.05$, $**p > 0.01$, $***p > 0.001$.
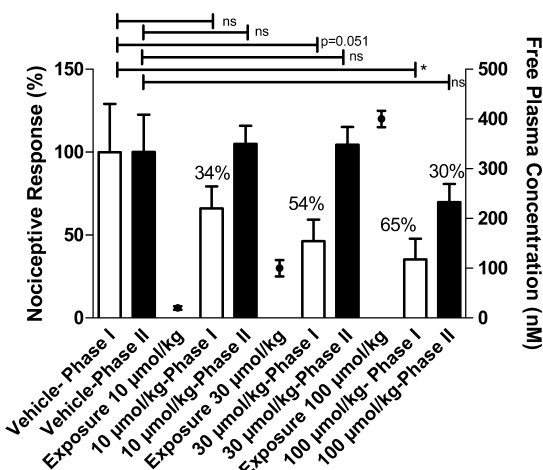

Figure 4. Dose response effect of **26B** in the rat formalin model. Compound is administered per oral gavage 15 min before formalin (100 μL of 2% solution) injection into the dorsal paw of Sprague−Dawley rats. Dose response effect is represented for both phases of the formalin test (phase I, 0−5 min; phase II, 15−35 min post formalin injection). The effect is expressed as the percentage in comparison to vehicle treated group ($n = 9$ per group), and free plasma concentration is expressed as mean ± SEM ($n = 9$ per group). Pairwise comparisons are used as t tests (Bonferroni) within a one-way ANOVA model per phase. No adjustment is performed for multiple comparisons. $*p < 0.05$.

Figure 5. Dose response effect of **16A** in the carrageenan monoarthritis model. The compound was administered per oral gavage 2 h 45 min post carrageen injection in the ankle joint of the rats. Behavioral measurement was performed, 15 min post compound administration, on a computerized set up developed internally called Paw Print. The effect is express as the percentage in comparison to vehicle treated group ($n = 9$ per group) and free plasma concentration is expressed as mean ± SEM ($n = 9$ per group). One-way ANOVA was used as statistic in comparison to vehicle group per phase, followed by followed by unpaired one-tailed t test.$*p < 0.05$.
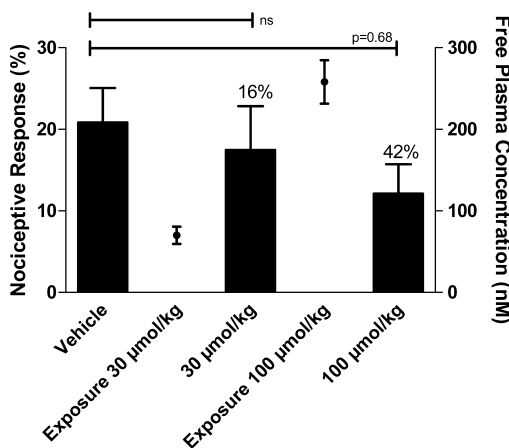
Figure 6. Dose response effect of **26B** in the carrageenan monoarthritis model. The compound was administered per oral gavage 2 h 45 min post carrageen injection in the ankle joint of the rats. Behavioral measurement was performed, 15 min post compound administration, on a computerized set up developed internally called Paw Print. The effect is express as the percentage in comparison to vehicle treated group ($n = 9$ per group) and free plasma concentration is expressed as mean ± SEM ($n = 9$ per group). One-way ANOVA was used as statistic in comparison to vehicle group per phase, followed by followed by unpaired one-tailed t test. $p = 0.068$.

carboxamides series described here, including compound **26B**, may be valuable for further investigations for pain therapeutics.

■ EXPERIMENTAL SECTION

Cell Lines and Culture Conditions. The recombinant HEK293 cell line expressing the human Na$_V$1.7 α-subunit and the Chinese hamster ovary (CHO) K1 cell line expressing the human Na$_V$1.2 α-subunit were obtained from Millipore. The human Na$_V$1.5 α-subunit and hERG expressing Chinese hamster ovary (CHO) K1 cell lines have

been described before.[43] The cDNA encoding the rat Na$_V$1.7 α-subunit (Genbank U79568) inserted into the pIRES-Neo2 vector was used to transfect HEK293 cells using the calcium phosphate method. Cells were selected with 400 μg/mL of G418, and single colonies were picked and characterized by patch-clamp electrophysiology. The cells were kindly donated by Mohamed Chahine (Department of Medicine and Laval Hospital, Laval University, QC, Canada). The human Na$_V$1.7 (F1737A) mutated cell line (clone 4) was generated by Lipofectamine 2000-mediated transfection of HEK293 cells with a point mutated expression construct briefly generated as follows. Two 152-bp long oligonucleotides (5′- GGGATGGATTGCTAGCACCTATTCTTAACAG-TAAGCCACCCGACTGTGACCCAAAAAAAGTTCATCCTG-

GAAGTTCAGTTGAAGGAGACTGTGGTAACCCATC) and (3′-TGACTGCAATGTACATGTTCACCACAACCAGGGCGGATAT-GATGATATAACTAACAAAGTAGAATATTCCAACAGATGGGT-TACCACAGTCTCCTTCAACTGA) containing the Phe to Ala codon were annealed and ligated to a Nhe1 and BsrGI digested SCN9A (database entry NM_002977) in pcDNA3.0. The mutated SCN9A cDNA was then transferred to pcDNA4.0/TO using the Kpn1and Xho1 restriction sites. The SCN9A inserts of all plasmid constructs were verified by sequencing of both strands. Cells were selected with Zeocin at 100 μg/mL, and single colonies were picked and characterized by Western Blotting and patch-clamp electrophysiology.

The Na$_V$1.7 cells were cultured in DMEM/F12+ Glutamax (Gibco) and the Na$_V$1.2 cells were cultured in IMDM + L-glutamate (Invitrogen), supplemented with 10% foetal bovine serum (Hyclone), 1% nonessential amino acids (Invitrogen), and 400 μg/mL Geneticin (Na$_V$1.7, and Na$_V$1.2 cells) or 100 μM Zeocine (Na$_V$1.7 [F1737A] cells) at 37 °C with 5% CO$_2$. Prior to electrophysiological recordings, the cells were incubated at 30 °C during the last 15−24 h, washed with Mg and Ca-free PBS, detached with trypsin, centrifuged and resuspended in D−PBS, and finally added to the IonWorks cell boat.

Electrophysiology. Sodium currents were recorded with the perforated whole-cell configuration of the patch-clamp from using the IonWorks Quattro planar patch clamp automated electrophysiology system (Molecular Devices, Inc.).[44]

The external recording solution (D-PBS, Gibco) contained (in mM) NaCl (138), KCl (2.7), KH$_2$PO$_4$ (1.5), Na$_2$HPO$_4$ (8), CaCl$_2$·2H$_2$O (0.9), MgCl$_2$·6H$_2$O (0.5), and glucose (5.5). The internal recording solution contained (in mM) K-gluconate (100), KCl (40), MgCl$_2$ (3), EGTA (3), and HEPES (5). pH was adjusted to 7.25 with KOH, and the final osmolarity was set at 290 mOsm. Amphotericin B was used as the perforating agent and added to the internal solution to give a final concentration of 150 μg/mL.

The compounds were analyzed using two different voltage protocols. The cells were either clamped to −90 mV, where the majority of channels are in a resting state, or they were clamped to −65 mV, which is referred to as the steady state. Comparing the two IonWorks protocols, as well as with manual patch clamp, we estimated the fraction of inactivated Na$_V$1.7 channels in the steady-state assay to be 40−50%. The sodium currents were evoked by a single voltage train consisting of eight 30 ms depolarizing steps to −20 mV (for Na$_V$1.7) and 10 mV (for Na$_V$1.2 and 1.5) from the holding potential at a frequency of 3 Hz. To recover a fraction of the channels from slow inactivation with the steady-state (V_{hold} −65 mV) protocol, a 20 ms hyperpolarizing step to −100 mV was executed prior to the activation step. The protocol was activated twice, prescan and postscan compound addition and the degree of inhibition for each well was assessed by dividing the two values for the eight pulse.

All compounds were dissolved in 100% dimethylsulfoxide (DMSO) to a final stock concentration of 10 mM. Half log serial dilutions were prepared in DMSO, where the final DMSO concentration in the external recording solution was 0.3%. The Na$_V$1.5 assay has been described before where a good correlation to manual electrophysiology was demonstrated for several known sodium channel blockers.[31] The hERG assay using IonWorks HT was performed as previously described.[45]

Some IC$_{50}$ values may be uncertain for compounds with low solubility, although the buffer conditions used for the functional assays and the solubility assay are not the same. All compounds were initially analyzed with an $n = 2$ at two different test occasions. The compounds selected for further profiling were analyzed with $n = 4−22$. Tetracaine was used as a reference compound present at every test occasion and showed mean IC$_{50}$ and SEM values of 0.11 ± 0.002 μM for Nav1.7 (V_{hold} −65 mV), 0.62 ± 0.017 μM for Nav1.7 (V_{hold} −90 mV), 0.53 ± 0.027 μM for Na$_V$1.5 (V_{hold} −90 mV), and 1.1 ± 0.12 μM for Nav1.2 (V_{hold} −65 mV).

Ex Vivo Electrophysiology. Three to four days after the SNL operation, animals were anesthetized with isoflurane. The L4 and L5 dorsal root ganglia (DRG) with attached dorsal roots and spinal nerve stumps were excised. The DRG were mounted in an in vitro recording chamber with one compartment for the DRG and the spinal nerve and an adjoining compartment for the dorsal root. The volume of DRG compartment is about 1 mL. The DRG and spinal nerve compartment was perfused with oxygenated (95% O$_2$−5% CO$_2$) artificial cerebrospinal fluid (ACSF) (in mM: 126 NaCl, 3 KCl, 2 MgSO$_4$, 26 NaHCO$_3$, 1.25 NaH$_2$PO$_4$, 10 glucose, 2 CaCl$_2$, pH 7.4) at a rate of 1.25−1.5 mL/min. The dorsal root compartment was filled with paraffin oil. The temperature was kept at 35 ± 0.5 °C through a temperature controlled water bath.

Single fiber recordings were performed, and ectopic discharges were recorded from teased dorsal root fascicles. Action potentials were amplified via a differential amplifier (DAM80, World Precision Instrument, USA) with a gain of ×1000 and filtered, with lower pass 10 kHz and high pass 10 Hz. Signals were digitized at 20 kHz by a data acquisition system (Power 1401, Cambridge Electronic Design, UK) and fed into a personal computer (Spike2, 5.01 software (Cambridge Electronic Design, UK), Microsoft Windows 2000 operating system), to allow sampling and offline analysis of the neuronal activity. Neuronal activity from single spike was monitored online by spike sorting function of data acquisition system and was further converted into a histogram.

Once stable baseline of ectopic discharge was established and recorded for at least 5 min, ACSF followed by three concentrations of a single compound were applied to the DRG compartment for 15 min each via a pump at a rate of 1.25−1.5 mL/min. Compound **28B** was diluted with ACSF from a 10 mM solution in DMSO prior to each experiment to final concentrations of 74, 222, and 740 nM.

The effect of the compound on the ectopic firing was analyzed through calculation of the mean frequency. For each fiber, 5 min baseline ectopic firing was averaged and used as a control. The ectopic activities during application of buffer (ACSF) and drugs were averaged every 3 min and then normalized to the percentage change of mean control frequency. The magnitude and time profile of inhibition were calculated. For a particular fiber, the ectopic firing was considered to be inhibited if the reduction of its firing frequency at the end of perfusion, i.e., the last 3 min, exceeded 50% of the control frequency. Fibers that fulfill this criterion were included for further analysis. Data are expressed as mean ± standard error of mean (SEM).

In Vivo Pharmacokinetics. Male Sprague−Dawley rats (Scanbur B&K AB, Sollentuna, Sweden) were housed with up to five animals per cage and were allowed to acclimatize to the new environment for at least one week upon arrival. In the conditioned animal facility, room temperature was kept at 20 ± 2 °C, relative humidity at 60 ± 20%, and a 12 h light−dark cycle was maintained including a 0.5 h dusk or dawn period (lights on at 6.30 a.m.). Water and standard rodent diet were freely accessible. All animal handling and experiments within AstraZeneca were performed in full compliance with authorial and ethical guidelines.

Rats (∼300 g) received 3 μmol/kg of the test compound intravenously as a bolus injection ($N = 3$) or 10 μmol/kg orally via gavage ($N = 3$). The formulations consisted of 1.5−5% DMA and 98.5−95% (HPbCD and 23.5 mg/mL glycerin in water). The content of HPbCD was adjusted dependent on the physicochemical properties of the test compounds. Serial blood samples (400 μL) from the tail vein were collected in microtainer tubes containing EDTA at 0.02, 0.08, 0.33, 0.67, 1, 3, 6, and 24 h following iv administration, or at 0.25, 0.5, 0.75, 1, 1.5, 2.5, 6, and 24 h following po administration. The blood samples were centrifuged, and plasma was transferred to a new tube. Sample preparation, bioanalysis with LC-MS/MS, and data analysis has been described previously.[46,47] Plasma protein binding in rat was determined using equilibrium dialysis.[48]

In Vivo Pharmacology. The rat formalin test was performed on male Sprague−Dawley rats from Scanbur B&K Universal, Sollentuna, Sweden (∼220 g). In brief, the rats were habituated to the experimental environment for 30 min prior to testing. The animals were randomly assigned to different experimental groups ($n = 9$ per group), and compounds **16A** or **26B** were administered per oral gavage 15 min before formalin injection. The formalin test is performed by injecting 100 μL of 2.0% formalin (in saline) subcutaneously on the dorsal side of the left hind paw. The behavior of the animals was recorded for 35 min after formalin injection, and time spent licking the injected paw was analyzed to represent nociceptive behavior. The response to formalin

injection was biphasic: phase I (0−5 min after formalin injection) and phase II (15−35 min after formalin injection).

Compound **16A** was dissolved in 10% hydropropylbetacyclodextrin in Milli-Q water at doses of 30, 100, and 140 μmol/kg, whereas compound **26B** was dissolved in 0.5% hydropropylmethylcellulose in 0.1% Tween 80 in water at doses 10, 30, and 100 μmol/kg.

The carrageenan-induced monoarthritis test was performed on male Sprague−Dawley rat (Harlan Laboratories BV, Netherlands; ∼220 g, n = 9 per group) as previously described.[49] In brief, under isoflurane anesthesia, 50 μL of carrageenan solution (7.5 mg/mL in saline, λ-carrageenan, Sigma Aldrich, Stockholm, Sweden) was injected into the ankle joint of the rats, inducing swelling and hyperalgesia. Two hours 45 minutes after the injection, compound **16A** or **26B** at doses of 0, 30, and 100 μmol/kg were administered per oral gavage. Behavioral measurement was performed, 15 min post compound administration, on a computerized set up developed internally called Paw Print. The observation of changes in gait is automatically measured and removes any operator bias. In brief, the set up consists of a pathway where rats were trained to go through. The glass floor of the pathway associated to light allowed detection of a light-print for each rat paw hitting the floor. The light intensity and the area of the print were dependent on the pressure applied by the rat paw. Each print on the glass floor was recorded via a camera, and gait pattern and weight bearing were extracted from the prints and analyzed by a computer-based system. Nociception as a result of the induced hyperalgesia was defined by a guarding index and represent the difference in weight bearing between the hind paws (in per mill (‰) of the total weight bearing on all limbs). A guarding index of 0 indicates that there is an equal amount of weight bearing on the both hind paws, and an increase in the guarding index indicates a shift of the weight bearing of the affected paw to the unaffected paw. At the end of the experiment, blood samples were collected by heart punction under isoflurane anesthesia prior to sacrifice.

Determination of Metabolic Stability. The microsome Cl_{int} values in rat and human were determined from the disappearance of the parent compound as described previously.[50] In short, 1 μM of the compound was incubated with 0.5 mg/mL of microsomes for 5, 15, 30, and 60 min in the presence of 1.5 mM NADPH. The reactions were stopped by the addition of 100 μL of acetonitrile and analyzed on LC-MS/MS. Control incubations (without microsomes) were performed for all compounds.

Chemistry: General. All materials were obtained from commercial supplier, unless otherwise noted, and used without further purification. Mass spectra were recorded either on Waters Alliance 2795 LC-MS (ZQ) with ESI, APCI, and APPI in both positive and negative ionization mode or Agilent GC-MS with chemical ionization (CI, methane as reactant gas). For separation, a capillary column was used, DB-5MS (J&W Scientific). A linear temperature gradient was applied. Preparative chromatography was run on a Waters FractionLynx system with a MS-triggered fraction collection (ESI). Column; XBridge Prep C8 5 μm OBD 19 mm × 100 mm, with guard column; XTerra Prep MS C8 10 μm 19 mm × 10 mm cartridge. A gradient from 100% A (95% 0.1 M ammonium acetate in Milli-Q water and 5% acetonitrile) to 100% B (100% acetonitrile) was applied for LC separation at a flow rate 25 mL/min. Purity for final compounds was greater than 95% unless otherwise noted and measured on one of the following instruments: (A) An Agilent HP1100 high performance liquid chromatography (HPLC) system with UV detections at 220, 254, and 290 nm. Phenomenex Gemini C18 3.0 mm × 50 mm, 3 μm, flow rate of 1.0 mL/min. A linear gradient was used starting at 100% A (A: 10 mM ammonium acetate in 5% acetonitrile) and ending at 100% B (B: acetonitrile) after 3.5 min. (B) A Waters Acquity UPLC system with UV detection at 254 nm was equipped with Waters ZQ mass spectrometer. Waters Acquity UPLC BEH C_8 2.1 mm × 50 mm, 1.7 μm, flow rate 1.0 mL/min. A linear gradient ranging from 5 to 95% CH_3CN in H_2O with 0.01 M ammonium acetate was used. The gradient was completed in 2 min 15 s. The ZQ mass spectrometer was run with ESI in positive and negative modes. High resolution mass spectra (HRMS) were recorded on a Waters Synapt-G2 mass spectrometer (Waters MS Technologies, Manchester, UK) connected to an Acquity UPLC system with a PDA detector (Waters Corp., Milford, USA). All analyses were acquired using

positive mode electrospray ionization (ESI+) in full scan and leucine encephalin (Sigma) was used as the lock mass (m/z 556.2771). Chromatographic separation was achieved with a 2.3 min gradient from 5 to 95% ACN (0.1% formic acid) over an Acquity UPLC BEH C18 1.7 μm, 2.1 mm × 50 mm column (Waters) maintained at 50 °C and run at a flow rate of 0.4 mL/min. NMR spectra were recorded on a Varian 400 MHz or on a Bruker 400 MHz and Bruker 500 MHz NMR spectrometer. The following reference signals were used: TMS δ 0.00, or the residual solvent signal of DMSO-d_6 δ 2.49, CD_3OD δ 3.31, or $CDCl_3$ δ 7.25 (unless otherwise indicated). Resonance multiplicities are denoted s, d, t, q, m, and br for singlet, doublet, triplet, quartet, multiplet, and broad, respectively. Unless otherwise stated, chemical shifts are given in ppm with the solvent as internal standard. Column chromatography was performed using Merck Silica gel 60 (0.040−0.063 mm), or employing a Combi Flash Companion system using RediSep normal-phase flash columns.

Preparation of Isoindoline Carboxamides via Ugi Reaction, General Procedure A. To the methanol (1 mL) solution of 2-formylbenzoic acid (**1**) (0.3 mmol, 1 equiv), the corresponding amine **2** (0.3 mmol, 1 equiv) in methanol (1 mL) was added followed by isocyanide **3** (0.3 mmol, 1 equiv). The mixture was stirred overnight at ambient temperature before it was filtered and purified using preparative liquid chromatography. The fractions containing the product were pooled, and the acetonitrile was removed in vacuum. The water solution was extracted with ethyl acetate. The organic layer was dried over magnesium sulfate and concentrated to yield the title compound as solid.

1-(Isocyanomethyl)-3-(trifluoromethoxy)benzene (3a). Step 1: The DCM solution (4 mL) of the commercially available 3-(trifluoromethoxy)phenyl)methanamine **6a** (0.2 g, 1.05 mmol) was set under N_2 atmosphere and cooled down to 0 °C. Thereafter, phenyl formate (0.117 mL, 1.05 mmol) was added dropwise via syringe and the mixture was stirred at room temperature for 16 h. The solvent was removed in vacuo, and the residue was purified on silica column using heptane:ethyl acetate = 100:0 to 0:100 as gradient, affording N-(3-(trifluoromethoxy)benzyl)formamide as colorless oil, 120 mg (52%). ^{1}H NMR (500 MHz, $CDCl_3$) δ 8.32 (s, 1 H), 7.38 (dd, J = 8.84, 7.71 Hz, 1 H), 7.25 (d, J = 7.71 Hz, 1 H), 7.19−7.11 (m, 2 H), 5.90 (br s, 1 H), 4.53 (d, J = 6.06 Hz, 2 H). MS (ESI) m/z 220 [M + H].

Step 2: N-(3-(Trifluoromethoxy)benzyl)formamide (0.120 g, 0.55 mmol) was dissolved in dichloromethane (4 mL) and cooled to −15 °C under N_2 atmosphere. N,N-Diisopropylethylamine (0.362 mL, 2.19 mmol) followed by phosphorus oxychloride (0.061 mL, 0.66 mmol) were added, and the resulting mixture was allowed to slowly reach room temperature. Then methanol (1.5 mL) was added to quench the reaction. The mixture was diluted with dichloromethane and washed twice with satd $NaHCO_3$ solution. The combined organic extracts were washed with brine, dried over anhydrous sodium sulfate, filtered, and evaporated to give the product as a brown oil, 110 mg (100%) which was used without further purification. ^{1}H NMR (500 MHz, $CDCl_3$) δ 7.49−7.43 (m, 1 H), 7.31 (d, J = 7.57 Hz, 1 H), 7.25−7.21 (m, 2 H), 4.69 (s, 2 H). MS (ESI) m/z 202 [M + H].

1-Fluoro-4-(isocyanomethyl)-2-(trifluoromethyl)benzene (3e). Step 1: N-(4-Fluoro-3-(trifluoromethyl)benzyl)formamide was prepared following the procedure described for intermediate **3a** in step 1, using (4-fluoro-3-(trifluoromethyl)phenyl)methanamine (446 mg, 2.31 mmol), triethylamine (0.644 mL, 4.62 mmol), and phenyl formate (0.302 mL, 2.77 mmol). The mixture was stirred under argon at room temperature for four days. The reaction mixture was purified by silica gel chromatography using EtOAc in heptane 0−90% as gradient, yielding the product as white solid, 338 mg (66.2%). ^{1}H NMR (400 MHz, $CDCl_3$) δ 8.32 (s, 1 H), 7.59−7.45 (m, 2 H), 7.23−7.14 (m, 1 H), 5.93 (br s, 1 H), 4.52 (d, J = 6.06 Hz, 2 H). GC-MS (CI) m/z 221 [M^+].

Step 2: Compound **3e** was prepared according to the method described for **3a** in step 2 from N-(4-fluoro-3-(trifluoromethyl)benzyl)-formamide (338 mg, 1.53 mmol), N,N-diisopropylethylamine (1.010 mL, 6.11 mmol), and phosphorus oxychloride (0.171 mL, 1.83 mmol). Afterward, the reaction mixture was concentrated, the residue was dissolved in methanol (3 mL), and triethylamine (2.5 mL) was added. The reaction mixture was stirred for 5 min and concentrated under

reduced pressure. The crude compound was purified by silica gel column chromatography using hexane:ethyl acetate = 100:0 to 80:20. The product was obtained as brown liquid, 293 mg (94%). ^{1}H NMR (400 MHz, CDCl$_3$) δ 7.65−7.54 (m, 2 H), 7.28 (t, J = 9.22 Hz, 1 H), 4.69 (s, 2 H). GC-MS (CI) m/z 203 [M$^+$].

N-(3,4-Dimethylphenyl)-3-oxo-2-(2-(pyridin-2-yl)ethyl)-isoindoline-1-carboxamide (10). The title compound was synthesized according to the general procedure A from 2-formylbenzoic acid (75 mg, 0.50 mmol), 2-(pyridin-2-yl)ethanamine (61.1 mg, 0.50 mmol), and 4-(isocyano)-1,2-dimethylbenzene (65.6 mg, 0.5 mmol). White solid, 101 mg (52%). ^{1}H NMR (400 MHz, DMSO-d_6) δ 10.57 (s, 3 H), 8.47−8.42 (m, 1 H), 7.73−7.66 (m, 2 H), 7.65−7.57 (m, 2 H), 7.55−7.48 (m, 1 H), 7.39 (d, J = 2.02 Hz, 1 H), 7.34 (dd, J = 8.08, 2.27 Hz, 1 H), 7.30 (d, J = 7.58 Hz, 1 H), 7.20 (ddd, J = 7.45, 4.93, 1.26 Hz, 1 H), 7.08 (d, J = 8.08 Hz, 1 H), 5.38 (s, 1 H), 4.29−4.19 (m, 1 H), 3.51−3.42 (m, 1 H), 3.12 (d, J = 7.33 Hz, 1 H), 3.09−3.00 (m, 1 H), 2.19 (s, 3 H), 2.17 (s, 3 H). MS (ESI) m/z 386 [M + H]. HRMS calcd for C$_{24}$H$_{23}$N$_3$O$_2$ (M + H)$^+$ 386.1869, found 386.1862.

3-Oxo-2-(2-pyridin-2-ylethyl)-N-[[4-(trifluoromethoxy)phenyl]-methyl]-1H-isoindole-1-carboxamide (16). The title compound was synthesized according to the general procedure A from 2-formylbenzoic acid (1 g, 6.6 mmol), 2-(2-aminoethyl)pyridine (814 mg, 6.6 mmol), and 1-(isocyanomethyl)-4-trifluoromethoxybenzene (1.34 g, 6.6 mmol). White solid, 1.83 g (60%). ^{1}H NMR (400 MHz, DMSO-d_6) δ 9.20 (t, J = 6.00 Hz, 1 H), 8.48−8.42 (m, 1 H), 7.72−7.64 (m, 2 H), 7.63−7.57 (m, 1 H), 7.57−7.48 (m, 2 H), 7.41−7.34 (m, 2 H), 7.34−7.28 (m, 2 H), 7.26 (d, J = 7.83 Hz, 1 H), 7.24−7.18 (m, 1 H), 5.24 (s, 1 H), 4.36 (d, J = 5.81 Hz, 2 H), 4.26−4.15 (m, 1 H), 3.46−3.36 (m, 1 H), 3.14−3.04 (m, 1 H), 3.04−2.94 (m, 1 H). MS (ESI) m/z 456 [M + H]. HRMS calcd for C$_{24}$H$_{20}$F$_3$N$_3$O$_3$ (M + H)$^+$ 456.1535, found 456.1537.

2-(Oxan-4-yl)-3-oxo-N-[[4-(trifluoromethoxy)phenyl]methyl]-1H-isoindole-1-carboxamide (26). The title compound was synthesized according to the general procedure A from 2-formylbenzoic acid (45 mg, 0.3 mmol), tetrahydro-2H-pyran-4-amine (30 µL, 0.30 mmol), and 1-(isocyanomethyl)-4-(trifluoromethoxy)benzene (57 mg, 0.29 mmol). White solid, 78 mg (60%). ^{1}H NMR (500 MHz, DMSO-d_6) δ 9.16 (t, J = 5.83 Hz, 1 H), 7.69 (d, J = 7.25 Hz, 1 H), 7.62−7.57 (m, 1 H), 7.53 (d, J = 7.57 Hz, 1 H), 7.51−7.47 (m, 1 H), 7.41−7.36 (m, 2 H), 7.35−7.30 (m, 2 H), 5.32 (s, 1 H), 4.34 (d, J = 5.67 Hz, 2 H), 4.16−4.07 (m, 1 H), 3.89 (dd, J = 11.35, 4.10 Hz, 1 H), 3.81 (d, J = 10.72 Hz, 1 H), 3.40−3.30 (m, 2 H), 1.90−1.79 (m, 1 H), 1.73−1.64 (m, 3 H). MS (ESI) m/z 435 [M + H]. HRMS calcd for C$_{22}$H$_{21}$F$_3$N$_2$O$_4$ (M + H)$^+$ 435.1532, found 435.1530.

2-(4,4-Difluorocyclohexyl)-3-oxo-N-[4-(trifluoromethoxy)benzyl]-isoindoline-1-carboxamide (28). The title compound was prepared according to the general procedure A with minor modification as follows. 4,4-Difluorocyclohexanaminium chloride (0.429 g, 2.50 mmol) was dissolved in methanol (10 mL), and 2-formylbenzoic acid (0.375 g, 2.5 mmol) was added. The mixture was set under argon atmosphere and then the pH was adjusted to ~6 by addition of triethylamine (1.045 mL, 7.50 mmol). After stirring for 5 min, 1-(isocyanomethyl)-4-(trifluoromethoxy)benzene (0.478 mL, 2.38 mmol) was added and the resulting mixture was stirred at ambient temperature for 16 h. The crude mixture was purified by silica gel chromathography using heptane:ethyl acetate = 100:0 to 50:50 as gradient. White solid, 430 mg (36.7%). ^{1}H NMR (500 MHz, CDCl$_3$) δ 7.71−7.64 (m, 1 H), 7.64−7.55 (m, 2 H), 7.52−7.41 (m, 1 H), 7.18−7.01 (m, 4 H), 6.32 (t, J = 6.31 Hz, 1 H), 5.11 (s, 1 H), 4.45 (dd, J = 14.74, 6.38 Hz, 1 H), 4.31 (dd, J = 14.82, 5.83 Hz, 1 H), 4.24−4.09 (m, 1 H), 2.25−2.02 (m, 2 H), 1.97−1.75 (m, 6 H). MS (ESI) m/z 469 [M + H]. HRMS calcd for C$_{23}$H$_{21}$F$_5$N$_2$O$_3$ (M + H)$^+$ 469.1551, found 469.1549.

2-(2-(5-Fluoropyrimidin-2-yl)ethyl)-3-oxo-N-(4-(trifluoromethoxy)benzyl)isoindoline-1-carboxamide (51). The title compound was prepared according to the modified procedure A, described for 28, using 2-(5-fluoropyrimidin-2-yl)ethanamine hydrochloride (59.2 mg, 0.33 mmol), triethylamine (0.093 mL, 0.67 mmol), 2-formylbenzoic acid (50 mg, 0.33 mmol), and 1-(isocyanomethyl)-4-(trifluoromethoxy)benzene (0.067 mL, 0.33 mmol). The mixture was stirred at 45 °C for 16 h. Yellow semisolid, 18 mg (11%). ^{1}H NMR (400 MHz, CDCl$_3$) δ 8.37 (s, 2 H), 8.17−8.00 (m, 1 H), 7.75−7.63 (m, 2 H),

7.59 (td, J = 7.52, 1.26 Hz, 1 H), 7.48 (t, J = 7.39 Hz, 1 H), 7.19−7.11 (m, 2 H), 7.11−7.03 (m, 2 H), 5.12 (s, 1 H), 4.42 (dd, J = 5.75, 1.71 Hz, 2 H), 4.18−4.03 (m, 1 H), 4.03−3.84 (m, 1 H), 3.37−3.19 (m, 2 H). MS (ESI) m/z 475 [M + H]. HRMS calcd for C$_{23}$H$_{18}$F$_4$N$_4$O$_3$ (M + H)$^+$ 475.1393, found 475.1394.

2-(2-(5-Fluoropyrimidin-2-yl)ethyl)-3-oxo-N-(3-(trifluoromethoxy)benzyl)isoindoline-1-carboxamide (60). The title compound was synthesized according to the general procedure A from 2-formylbenzoic acid (112 mg, 0.74 mmol), 2-(5-fluoropyrimidin-2-yl)ethanamine (105 mg, 0.74 mmol), and 1-isocyano-3-(trifluoromethoxy)benzene 3a (139 mg, 0.74 mmol). The reaction mixture was stirred at 40 °C overnight. The mixture was purified by silica gel chromatography using EtOAc in heptane 0−100% as gradient. The product was obtained as semisolid, 187 mg (53%). ^{1}H NMR (400 MHz, CD$_3$OD) δ 8.64−8.50 (m, 2 H), 7.73 (dt, J = 7.20, 1.20 Hz, 1 H), 7.65−7.57 (m, 1 H), 7.57−7.50 (m, 2 H), 7.43−7.35 (m, 1 H), 7.26 (ddd, J = 7.83, 1.33, 1.20 Hz, 1 H), 7.22−7.09 (m, 2 H), 5.28 (s, 1 H), 4.50−4.38 (m, 3 H), 3.69 (dt, J = 14.27, 6.38 Hz, 1 H), 3.37−3.33 (m, 1 H), 3.30−3.23 (m, 1 H). MS (ESI) m/z 475 [M + H]. HRMS calcd for C$_{23}$H$_{18}$F$_4$N$_4$O$_3$ (M + H)$^+$ 475.1393, found 475.1402.

N-(4-Fluoro-3-(trifluoromethyl)benzyl)-2-(2-(5-fluoropyrimidin-2-yl)ethyl)-3-oxoisoindoline-1-carboxamide (62). The title compound was prepared according to the modified procedure A, described for 28, using 2-(5-fluoropyrimidin-2-yl)ethanamine hydrochloride (126 mg, 0.71 mmol), triethylamine (0.123 mL, 0.89 mmol), 2-formylbenzoic acid (89 mg, 0.59 mmol), and 1-fluoro-4-(isocyanomethyl)-2-(trifluoromethyl)benzene 3e (0.120 mL, 0.59 mmol). The mixture was stirred at 45 °C for 48 h. White solid, 41 mg, (14.6%). ^{1}H NMR (500 MHz, CDCl$_3$) δ 8.42 (s, 2 H), 8.21−8.13 (m, 1 H), 7.67 (d, J = 8.35 Hz, 1 H), 7.62−7.55 (m, 2 H), 7.50−7.41 (m, 1 H), 7.36−7.28 (m, 2 H), 7.10−7.01 (m, 1 H), 5.11 (s, 1 H), 4.51 (dd, J = 14.98, 6.31 Hz, 1 H), 4.37 (dd, J = 14.98, 5.67 Hz, 1 H), 4.14−4.05 (m, 1 H), 4.05−3.95 (m, 1 H), 3.32−3.22 (m, 2 H). MS (APP−) m/z 475 [M − H]. HRMS calcd for C$_{23}$H$_{17}$F$_5$N$_4$O$_2$ (M + H)$^+$ 477.1350, found 477.1344.

■ ASSOCIATED CONTENT

⑤ Supporting Information
Experimental procedures for **10−63** and their precursors. Additional characterization data of **16**, **26**, **28**, **51**, **60**, and **62**. This material is available free of charge via the Internet at http://pubs.acs.org.

■ AUTHOR INFORMATION

Corresponding Author
*Phone: +46 8 553-24322. E-mail: istvan.macsari@astrazeneca.com.

Notes
The authors declare no competing financial interest.

■ ACKNOWLEDGMENTS

■ ABBREVIATIONS USED

Na$_V$1.7, voltage-gated sodium channel type 7; Na$_V$1.5, voltage-gated sodium channel type 5; Na$_V$1.2, voltage-gated sodium channel type 2; SCN9A, sodium channel, voltage-gated, type IX, R subunit; SAR, structure−activity relationship; DIPEA, N,N-diisopropylethylamine; THF, tetrahydrofuran; DCM, dichloromethane; DMF, N,N-dimethylformamide; NBS, N-bromosuccinimide; AIBN, 2,2′-azobis(2-methylpropionitrile); hERG, human ether a-go-go-related gene; LLE, lipophilic ligand efficiency; PK, pharmacokinetic; Cl$_{int}$, in vitro intrinsic clearance; RLM, rat liver microsome; HLM, human liver microsome; AUC,

area under curve; V_{ss}, volume of distribution; $t_{1/2}$, terminal half-life; CL, systemic clearance; C_{max}, maximal concentration; T_{max}, time at which maximal concentration is measured; F, oral bioavailability; f_u, unbound fraction; DRG, dorsal root ganglion; hCav3.2, T type voltage-dependent calcium channel, α 1H subunit; hIKs, intermediate-conductance calcium-activated potassium channel, known as $K_{Ca}3.1$; $hK_V1.5$, voltage-gated potassium channel type 5; hKCNQ2, potassium voltage-gated channel, KQT-like subfamily, member 2; hTRPA1, transient receptor potential cation channel, subfamily A, member 1; GPCR, G-protein-coupled receptor

■ REFERENCES

(1) Catterall, W. A; Goldin, A. L.; Waxman, S. G. International Union of Pharmacology. XLVII. Nomenclature and structure− function relationships of voltage-gated sodium channels. *Pharmacol. Rev.* **2005**, *57*, 397−409.

(2) Ahmad, S.; Dahllund, L.; Eriksson, A. B.; Hellgren, D.; Karlsson, U.; Lund, P.-E.; Meijer, I. A.; Meury, L.; Mills, T.; Moody, A.; Morinville, A.; Morten, J.; O'Donnell, D.; Raynoschek, C.; Salter, H.; Rouleau, G. A.; Krupp, J. J. A stop codon mutation in SNC9A causes lack of pain sensation. *Hum. Mol. Genet.* **2007**, *16*, 2114−2121.

(3) Cox, J. J.; Reimann, F.; Nicholas, A. K.; Thornton, G.; Roberts, E.; Springell, K.; Karbani, G.; Jafri, H.; Mannan, J.; Raashid, Y.; Al Gazali, L.; Hamamy, H.; Valente, E. M.; Gorman, S.; Williams, R.; McHale, D. P.; Wood, J. N.; Gribble, F. M.; Woods, C. G. An SCN9A channelopathy causes congenital inability to experience pain. *Nature* **2006**, *444*, 894−898.

(4) Goldberg, Y. P.; MacFarlane, J.; MacDonald, M. L.; Thompson, J.; Dube, M. P.; Mattice, M.; Fraser, R.; Young, C.; Hossain, S.; Pape, T.; Payne, B.; Radomski, C.; Donaldson, G.; Ives, E.; Cox, J.; Younghusband, H. B.; Green, R.; Duff, A.; Boltshauser, E.; Grinspan, G. A.; Dimon, J. H.; Sibley, B. G.; Andria, G.; Toscano, E.; Kerdraon, J.; Bowsher, D.; Pimstone, S. N.; Samuels, M. E.; Sherrington, R.; Hayden, M. R. Loss-of-function mutations in the $Na_V1.7$ gene underlie congenital indifference to pain in multiple human populations. *Clin. Genet.* **2007**, *71*, 311−319.

(5) Staud, R.; Price, D. D.; Janicke, D.; Andrade, E.; Hadjipanayis, A. G.; Eaton, W. T.; Kaplan, L.; Wallace, M. R. Two novel mutations of SCN9A ($Na_V1.7$) are associated partial congenital insensitivity to pain. *Eur. J. Pain* **2011**, *15*, 223−230.

(6) Yang, Y.; Wang, Y.; Li, S.; Xu, Z.; Li, H.; Ma, L.; Fan, J.; Bu, D.; Liu, B.; Fan, Z.; Wu, G.; Jin, J.; Ding, B.; Zhu, X.; Shen, Y. Mutations in SCN9A, encoding a sodium channel alpha subunit, in patients with primary erythermalgia. *J. Med. Genet.* **2004**, *41*, 171−174.

(7) Drenth, J. P.; te Morsche, R. H.; Guillet, G.; Taieb, A.; Kirby, R. L.; Jansen, J. B. SCN9A mutations define primary erythermalgia as a neuropathic disorder of voltage gated sodium channels. *J. Invest. Dermatol.* **2005**, *124*, 1333−1338.

(8) Fertleman, C. R.; Baker, M. D.; Parker, K. A.; Moffatt, S.; Elmslie, F. V.; Abrahamsen, B.; Ostman, J.; Klugbauer, N.; Wood, J. N.; Gardiner, R. M.; Rees, M. SCN9A mutations in paroxysmal extreme pain disorder: allelic variants underlie distinct channel defects and phenotypes. *Neuron* **2006**, *52*, 767−774.

(9) Rogers, M.; Tang, L.; Madge, D. J.; Stevens, E. B. The role of sodium channels in neuropathic pain. *Semin. Cell Dev. Biol.* **2007**, *17*, 571−581.

(10) Zuliani, V.; Rivara, M.; Fantini, M.; Constantino, G. Sodium channel blockers for neuropathic pain. *Expert Opin. Ther. Pat.* **2010**, *20*, 755−779.

(11) Kemp, M. I. Structural trends among second-generation voltage-gated sodium channel blockers. *Prog. Med. Chem.* **2010**, *49*, 81−111.

(12) Bregman, H.; Berry, L.; Buchanan, J. L.; Chen, A.; Du, B.; Feric, E.; Hierl, M.; Huang, L.; Immke, D.; Janosky, B.; Johnson, D.; Li, X.; Ligutti, J.; Liu, D.; Malmberg, A.; Matson, D.; McDermott, J.; Miu, P.; Nguyen, H. N.; Patel, V. F.; Waldon, D.; Wilenkin, B.; Zheng, X. M.; Zou, A.; McDonough, S. I.; DiMauro, E. F. Identification of a potent,

state-dependent inhibitor of $Na_V1.7$ with oral efficacy in the formalin model of persistent pain. *J. Med. Chem.* **2011**, *54*, 4427−4445.

(13) Chowdhury, S.; Chafeev, M.; Liu, S.; Sun, J.; Raina, V.; Chui, R.; Young, W.; Kwan, R.; Fu, J.; Cadieux, J. A. Discovery of XEN907, a spirooxindole blocker of $Na_V1.7$ for the treatment of pain. *Bioorg. Med. Chem. Lett.* **2011**, *21*, 3676−3681.

(14) Macsari, I.; Sandberg, L.; Besidski, Y.; Gravenfors, Y.; Ginman, T.; Bylund, J.; Bueters, T.; Eriksson, A. B.; Lund, P.-E.; Venyike, E.; Arvidsson, P. I. Phenyl isoxazole voltage-gated sodium channel blockers: structure and activity relationship. *Bioorg. Med. Chem. Lett.* **2011**, *21*, 3871−3876.

(15) Nguyen, H. N.; Bregman, H.; Buchanan, J. L.; Du, B.; Feric, E.; Huang, L.; Li, X.; Ligutti, J.; Liu, D.; Malmberg, A. B.; Matson, D. J.; McDermott, J. S.; Patel, V. F.; Wilenkin, B.; Zou, A.; McDonough, S. I. Discovery and optimization of aminopyrimidinones as potent and state-dependent $Na_V1.7$ antagonists. *Bioorg. Med. Chem. Lett.* **2012**, *22*, 1055−1060.

(16) Bregman, H.; Nguyen, H. N.; Feric, E.; Ligutti, J.; Liu, D.; McDermott, J. S.; Wilenkin, B.; Zou, A.; Huang, L.; Li, X.; McDonough, S. I.; DiMauro, E. F. The discovery of aminopyrazines as novel, potent $Na_V1.7$ antagonists: hit-to-lead identification and SAR. *Bioorg. Med. Chem. Lett.* **2012**, *22*, 2033−2042.

(17) Chakka, N.; Bregman, H.; Du, B.; Nguyen, H. N.; Buchanan, J. L.; Feric, E.; Ligutti, J.; Liu, D.; McDermott, J. S.; Zou, A.; McDonough, S. I.; DiMauro, E. F. Discovery and hit-to-lead optimization of pyrrolopyrimidines as potent, state-dependent $Na_V1.7$ antagonists. *Bioorg. Med. Chem. Lett.* **2012**, *22*, 2052−2062.

(18) Gonzalez, J. E.; Termin, A. P.; Wilson, D. M. Small Molecule Blockers of Voltage-Gated Sodium Channels. Methods and Principles in Medicinal Chemistry. In *Voltage-Gated Ion Channels as Drug Targets*; Triggle, D. J., Gopalakrishnan, M., Rampe, D., Zheng, W., Mannhold, R., Kubinyi, H., Folkers, G., Eds.; Wiley-VCH: Weinheim, Germany, 2006; Vol. 29, pp 168−192.

(19) Priest, B. T. Future potential and status of selective sodium channel blockers for the treatment of pain. *Curr. Opin. Drug Discovery Dev.* **2009**, *12*, 682−692.

(20) Arvidsson, P. I.; Besidski, Y.; Csjernyik, G; Lange, T.; Macsari, I.; Nilsson, L. I. Isoindoline derivatives comprising an additional heterocyclic group and their use in the treatment of pain disorders. WO2009145718, 2009.

(21) Åhlin, K.; Arvidsson, P. I.; Besidski, Y.; Nilsson, L. I. Isoindoline derivatives comprising a cyano group and their use in the treatment of pain disorders. WO2009145719, 2009.

(22) Arvidsson, P. I.; Besidski, Y.; Csjernyik, G.; Sandberg, L. Isoindoline derivatives comprising additional heterocyclic groups and their use in the treatment of pain disorders. WO2009145720, 2009.

(23) Besidski, Y.; Claesson, A.; Csjernyik, G.; Macsari, I.; Nilsson, L. I. Isoindoline derivatives comprising phenyl groups and their use in the treatment of pain disorders. WO2009145721, 2009.

(24) Kato, S.; Nonoyama, N.; Tomimoto, K.; Mase, T. Noncryogenic metalation of aryl bromides bearing proton donating groups: formation of a stable magnesio-intermediate. *Tetrahedron Lett.* **2002**, *43*, 7315−7317.

(25) Nguyen, T.-H.; Chau, N. T. T.; Castanet, A.-S.; Nguyen, K. P. P.; Mortier., J. First General, Direct, and Regioselective Synthesis of Substituted Methoxybenzoic Acids by Ortho Metalation. *J. Org. Chem.* **2007**, *72*, 3419−3429.

(26) Othman, M.; Decroix, B. Synthesis of phthalimidine-3-carboxylate and benzopyrroloindolizine from N-(pyrrol-2-yl)-phthalimidine-3-carboxylate. *Synth. Commun.* **1996**, *26*, 2803−2809.

(27) Trivedi, S.; Dekermendjian, K.; Julien, R.; Huang, J.; Lund, P.-E.; Krupp, J.; Kronqvist, R.; Larsson, O.; Bostwick, R. Cellular HTS assays for pharmacological characterization of $Na_V1.7$ modulators. *Assay Drug Dev. Technol.* **2008**, *6*, 167−179.

(28) Xu, Z-Q. D.; Zhang, X.; Grillner, S.; Hökfelt, T. Electrophysiological studies on rat dorsal root ganglion neurons after peripheral axotomy: Changes in responses to neuropeptides. *Proc. Natl. Acad. Sci. U.S.A.* **1997**, *94*, 13262−13266.

(29) Liu, C.-N.; Michaelis, M.; Amir, R.; Devor, M. Spinal nerve injury enhances subthreshold membrane potential oscillations in DRG neurons: relation to neuropathic pain. *J. Neurophysiol.* **2000**, *84*, 205−215.

(30) Harmer, A. R.; Valentin, J.-P.; Pollard, C. E. On the relationship between block of the cardiac Na^+ channel and drug-induced prolongation of the QRS complex. *Br. J. Pharmacol.* **2011**, *164*, 260−273.

(31) Harmer, A. R; Abi-Gerges, N.; Easter, A.; Woods, A.; Lawrence, C. L.; Small, B. G.; Valentin, J.-P.; Pollard, C. E. Optimisation and validation of a medium-throughput electrophysiology-based $hNa_V1.5$ assay using IonWorks. *J. Pharmacol. Toxicol. Methods* **2008**, *57*, 30−41.

(32) Goldin, A. L. Resurgence of sodium channel research. *Annu. Rev. Physiol.* **2001**, *63*, 871−894.

(33) Tfelt-Hansen, J.; Winkel, B. G.; Grunnet, M.; Jespersen, T. Inherited cardiac diseases caused by mutations in the $Na_V1.5$ sodium channel. *J. Cardiovasc. Electrophysiol.* **2010**, *21*, 107−115.

(34) Alelyunas, Y. W.; Liu, R.; Pelosi-Kilby, L.; Shen, C. Application of a dried-DMSO rapid throughput 24 h equilibrium solubility in advancing discovery candidates. *Eur. J. Pharm. Sci.* **2009**, *37*, 172−182 The method was modified by a pre-incubation step for 4 h at a fixed temperature of 1°C with magnetic stirrers at 500 rpm in order to generate the most stable solid form..

(35) Dick, I. E.; Brochu, R. M.; Purohit, Y.; Kaczorowski, G. J.; Martin, W. J.; Priest, B. T. Sodium channel blockade may contribute to the analgesic efficacy of antidepressants. *J. Pain* **2007**, *8*, 315−324.

(36) Assays performed at MDS Pharma Services for compound **16A** and **26B** with no inhibition at 10 μM: cholinesterase ACES, cyclooxygenase COX-1, monoamine oxidase MAO-A, endothelial nitric oxide synthase eNOS, phosphodiesterase PDE4, insulin receptor protein tyrosine kinase, $adrenergic_{\alpha1D}$, $adrenergic_{\alpha2A}$, $adrenergic_{\beta1}$, calcium channel L-type benzothiazepine, dihydropyridine sites, dopamine $receptor_{D2L}$, estrogen ERα, GABA-A flunitrazepam, histamine receptor H1, muscarinic receptor M2, nicotinic acetylcholine, opiate receptor μ, serotonin receptor $5-HT_{2A}$, and norepinephrine transporter NET.

(37) Nau, C.; Wang, G. K. Interactions of local anesthetics with voltage-gated Na^+ channels. *J. Membr. Biol.* **2004**, *201*, 1−8.

(38) Li, H. L.; Galue, A.; Meadows, L.; Ragsdale, D. S. A molecular basis for the different local anesthetic affinities of resting versus open and inactivated states of the sodium channel. *Mol. Pharmacol.* **1999**, *55*, 134−141.

(39) Wang, G. K.; Russell, C.; Wang, S.-Y. State-dependent block of voltage-gated Na^+ channels by amitriptyline via the local anesthetic receptor and its implication for neuropathic pain. *Pain* **2004**, *110*, 166−174.

(40) Lebrun, P.; Manil, J.; Colin, F. Formalin-induced central sensitisation in the rat: somatosensory evoked potential data. *Neurosci. Lett.* **2000**, *283*, 113−116.

(41) Kortekangas, P.; Peltola, O.; Toivanen, A.; Aro, H. T. Synovial fluid L-lactic acid in acute arthritis of the adult knee joint. *Scand. J. Rheumatol.* **1995**, *24*, 98−101.

(42) Gerster, J. C.; Gobelet, C. Synovial fluid lactic acid in acute and chronic pyrophosphate arthropathy and in osteoarthritis. *Clin. Rheumatol.* **1988**, *7*, 197−199.

(43) Persson, F.; Carlsson, L.; Duker, G.; Jacobson, I. Blocking characteristics of hERG, $hNa_V1.5$, and hKvLQT1 hminK after administration of the novel anti-arrhythmic compound AZD7009. *J. Cardiovasc. Electrophysiol.* **2005**, *16*, 329−341.

(44) Schroeder, K.; Neagle, B.; Trezise, D. J.; Worley, J. Ionworks HT: A New High-Throughput Electrophysiology Measurement Platform. *J. Biomol. Screening* **2003**, *8*, 50−64.

(45) Bridgland-Taylor, M. H.; Hargreaves, A. C.; Easter, A.; Orme, A.; Henthorn, D. C.; Ding, M.; Davis, A. M.; Small, B. G.; Heapy, C. G.; Abi-Gerges, N.; Persson, F.; Jacobson, I.; Sullivan, M.; Albertson, N. Optimisation and validation of a medium-throughput electrophysiology-based hERG assay using IonWorks HT. *J. Pharmacol. Toxicol. Methods* **2006**, *54*, 189−199.

(46) Bueters, T.; Dahlström, J.; Kvalvågnaes, K.; Betner, I.; Briem, S. High-throughput analysis of standardized pharmacokinetic studies in the rat using sample pooling and UPLC-MS/MS. *J. Pharm. Biomed. Anal.* **2011**, *55*, 1120−1126.

(47) Briem, S.; Martinsson, S.; Bueters, T.; Skoglund, E. Combined approach for high-throughput preparation of plasma samples from exposure studies. *Rapid Commun. Mass Spectrom.* **2007**, *21*, 1965−1972.

(48) Borgegard, T.; Juréus, A.; Olsson, F.; Rosqvist, S.; Sabirsh, A.; Rotticci, D.; Paulsen, K.; Klintenberg, R.; Yan, H.; Waldman, M.; Stromberg, K.; Nord, J.; Johansson, J.; Regner, A.; Parpal, S.; Malinowsky, D.; Radesater, A. C.; Li, T.; Singh, R.; Eriksson, H.; Lundkvist, J. First and second generation γ-secretase modulators (GSMs) modulate amyloid-β (Aβ) peptide production through different mechanisms. *Alzheimer's Dis. Res. J.* **2012**, *3*, 29−45.

(49) Finn, A.; Oerther, S. Can L(+)-lactate be used as a marker of experimentally induced inflammation in rats? *Inflammation Res.* **2010**, *59*, 315−321.

(50) Sohlenius-Sternbeck, A. K.; Afzelius, L.; Prusis, P.; Neelissen, J.; Hoogstraate, J.; Johansson, J.; Floby, E.; Bengtsson, A.; Gissberg, O.; Sternbeck, J.; Petersson, C. Evaluation of the human prediction of clearance from hepatocyte and microsome intrinsic clearance for 52 drug compounds. *Xenobiotica* **2010**, *40*, 637−649.